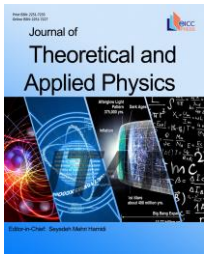

Volume 19, Issue 6, 192554 (1-11)

Journal of Theoretical and Applied Physics (JTAP)

https://doi.org/10.57647/j.jtap.2025.1906.54

Nuclear Density Distributions and Magnetic Moment of Mirror Nuclei ^{17}Ne and ^{17}N

Ghufran M. Sallh[1] and Ahmed N. Abdullah[2] *

[1]*Department of Physics, College of Science, University of Baghdad, Ibn Sina university, Baghdad Iraq*
[2]*Department of Physics, College of Science, University of Baghdad, Baghdad- Iraq*

***Corresponding author:** Ahmed.n@sc.uobaghdad.edu.iq

Original Research

Received:
23 May 2025

Revised:
12 Septembre2025

Accepted:
15 October 2025

Publish online:
31 December 2025

Abstract

The ground-state characteristics nuclear density distributions and root-mean-square (rms) radii of the exotic mirror nuclei ^{17}Ne and ^{17}N were examined using the Skyrme-Hartree-Fock method and the symmetrized Woods-Saxon (SWS) model. Additional nuclear properties, including elastic electron-scattering form factors, binding energies, Coulomb displacement energies, and magnetic dipole moments, were also investigated. The magnetic dipole moments were calculated within the ZBM shell-model framework using several interactions (ZWM, REWIL, ZBMII, and ZBMI), with the NuShellX@ code employed to compute one-body density matrix (OBDM) elements and halo-specific form factors. The extended tail behavior observed in the nuclear densities, indicative of halo structures, was consistent with experimental observations. Furthermore, elastic form factors including the monopole (C_0) component were derived from charge density distributions within the Plane-Wave Born Approximation (PWBA), offering predictive insight for forthcoming experiments involving electron–radioactive ion beam scattering.

Keywords: Mirror nuclei; Root mean square; Electron scattering; Coulomb displacement energy

1. Introduction

The investigation of short-lived nuclei far from β-stability has become a central topic in nuclear physics due to their exotic properties [1]-[4] .The proton drip-line nucleus ^{17}Ne was examined using a three-body model composed of 15O and two protons, revealing a proton radius 0.26–0.32 fm larger than that of the neutron, indicating a proton skin .Density distributions are critical for constructing microscopic optical potentials, analyzing elastic nucleus–nucleus scattering, and identifying weakly bound nuclear structures. Additionally, the scattering cross-section is highly sensitive to these density profiles [5].

Nuclear halos are a quantum effect that arising from the very weak binding of the valence nucleons and their occupation on the orbits have l = 0, 1 (low angular momentum), so that the wave functions of these valence nucleons have an extended radial dimension [6]. The presence of a low-density tail at large radial distances is a major feature of the density distribution of nuclear matter in halo nuclei [7] . Charge densities offer valuable insights into the internal structure of atomic nuclei, as they are closely linked to proton wave functions, which play a fundamental role in various nuclear physics calculations. The study of elastic electron scattering from nuclei has generated a vast amount of experimental data, enabling the assessment of nuclear ground state models. This field has evolved from initial estimations of root-mean-square (rms) charge radii to significantly more precise measurements in the 1970s and 1980s, leading to nearly model-independent determinations of charge density distributions for numerous nuclei [8]. The charge density distributions of stable nuclei have been extensively examined using this technique [9]. Despite the lack of prior studies on electron scattering for unstable nuclei, nuclear physicists aim to explore their structures through electron-nucleus scattering. While previous studies have investigated halo nuclei using a variety of density models and form factor analyses, relatively few have focused on a comprehensive comparative study of the mirror nuclei ^{17}Ne and ^{17}N

employing both the Skyrme-Hartree-Fock (SHF) method and the Symmetrized Woods-Saxon (SWS) model. Furthermore, experimental data on unstable nuclei remain sparse, especially regarding electron scattering observables. This work fills that scientific gap by offering a detailed comparison between neutron-rich and proton-rich mirror nuclei, illustrating how isospin asymmetry and Coulomb repulsion influence the extended distributions of nuclear matter and magnetic dipole moments. The adoption of two independent theoretical approaches enhances the predictive reliability of the results, which is crucial for interpreting future experimental findings in the field of exotic nuclei physics [9].

Mirror nuclei, with the proton and neutron numbers exchanged can have similar nuclear structures because of the isospin symmetry of nuclear forces [10]. The Coulomb displacement energy is the difference between binding energy of the mirror nuclei [11]. Mohammed et al. [12] studied the ground state density distributions, elastic form factors, and root mean square radii of pairs nuclei ^{17}Ne-^{17}N and ^{23}Al-^{23}Ne using the shell-model calculations with interactions and compared with available experimental data. For ^{17}Ne-^{17}N nuclei, p-shell and mixing of psd orbits were adopted with Cohen-Kurath (ckii) and psdsu3 interactions. While for ^{23}Al-^{23}Ne, the sd-shell and sdpf shell were adopted with the universal shell model (USD) and sdpfwa interactions. In general, it was found that the rms radius of the valence proton (s) is larger than that of the valence neutron (s) in its mirror nucleus. The results show that these nuclei have the exotic structure of a halo or skin.

The Magnetic dipole moments are fundamental physical quantities that provide a precise window into the internal structure of atomic nuclei and the angular distribution of nucleons. A nucleus's magnetic moment arises from the combined contributions of the orbital angular momentum and intrinsic spin (spin angular momentum) of both protons and neutrons. The total nuclear magnetic moment is expressed in units of the nuclear magneton (μ_N) and depends on the spatial distribution of nucleons, the nature of the occupied orbitals [13]. Phenomena such as the neutron skin and proton skin serve as key structural indicators of nucleon asymmetry in unstable nuclei. A neutron skin typically appears in neutron-rich nuclei due to the spatial extension of neutron density beyond the nuclear core, while a proton skin may emerge in proton-rich nuclei near the drip line, such as ^{17}Ne, where weakly bound outer protons extend further than the neutron distribution. These skin structures are often accompanied by a long density tail a low-density extension in the radial matter distribution that is characteristic of halo or skin-type nuclei. In such systems, valence nucleons occupy orbitals with low angular momentum and weak binding, allowing them to spread over large distances outside the nuclear core. These features have a significant impact on nuclear observables such as root-mean-square radii, elastic scattering form factors, and multipole moments. The presence of extended tails and skin structures plays a crucial role in identifying and characterizing halo and near-halo systems, particularly in light, exotic nuclei [14].

Mahdi et al. [15] investigated the ground-state properties of exotic ^{18}N and ^{20}F nuclei, including the neutron, proton and matter densities and related radii using the two-body model of within Gaussian (GS) and Woods Saxon (WS) wave functions. The long tail was evident in the computed neutron and matter densities of these nuclei.

The plane wave Born approximation (PWBA) was calculate the elastic form factors of these exotic nuclei. The variation in the proton density distributions due to the presence of the extra neutrons in ^{18}N and ^{20}F leads to a major difference between the elastic form factors of these exotic nuclei and their stable isotopes ^{14}N and ^{19}F. The reaction cross sections for these nuclei were investigated using the Kox and Glauber models.

The calculated results for the selected exotic nuclei are in a good agreement with the experimental data. Hadi et al. [16] employed the effective f5pvh interactions and the NuShellX@MSU code within the fp-shell to calculate the energy levels and electromagnetic transition probabilities of the ^{72,74,76} Kr nucleus. The use of the nuclear shell model utilizing the f5pvh interaction within the fp-shell demonstrates success, as evidenced by the concordance with both experimental and theoretical data.

In the present study, the ground-state properties like the nuclear densities and the rms radii for exotic mirror nuclei ^{17}Ne and ^{17}N will be investigated using the Skyrme-Hartree-Fock (SHF) and symmetrized Woods-Saxon (SWS) calculations. The elastic form factors, the binding energy, Coulomb displacement energy as well as the magnetic dipole (μ) moments for these exotic mirror nuclei will be also studied.

2. Theoretical Formulations

For halo nuclei, it is appropriate to model core and halo densities independently; thus, their ground-state matter density can be formulated as follows [17]:

$$\rho_m(r) = \rho_c(r) + \rho_v(r) \tag{1}$$

The ground-state densities of exotic halo nuclei have been computed using two methods: Skyrme-Hartree-Fock (SHF) and symmetrized Woods-Saxon (SWS), where the core and halo $\rho_c(r)$ and halo $\rho_v(r)$ densities are given by:

$$\rho_c(r) = \frac{1}{4\pi}\sum_{n\ell j} N_c^{n\ell j}\left|R_{n\ell j}(r)\right|^2 \tag{2}$$

$$\rho_v(r) = \frac{1}{4\pi} N_h^{n\ell j}\left|R_{n\ell j}(r)\right|^2 \tag{3}$$

where $R_{n\ell j}(r)$ and $N^{n\ell j}$ denote the radial wave function and the occupation number of the orbit $n\ell j$, respectively.

The $R_{n\ell j}(r)$ obtained by solving the radial part of the Schrödinger equation using the potential of SWS [18]:

In the SWS method, the core and halo densities are calculated by solving the eigenvalue problem of Symmetrized Woods-Saxon potential:

$$\frac{d^2R_{n\ell j}(r)}{dr^2}+\frac{2m}{\hbar^2}\left[\varepsilon_{n\ell j}-V(r)-\frac{\hbar^2}{2m}\frac{\ell(\ell+1)}{r^2}\right]R_{n\ell j}(r)=0 \quad (4)$$

where $\varepsilon_{n\ell j}$ is the single-particle binding energy and the $V(r)$ is the core potential given as:

$$V(r)=V_0(r)+V_{so}(r)\,L.S+V_c(r) \quad (5)$$

$V_0(r)$ is the central potential takes the SWS from [19]:

$$V_0(r)=-V_0\,\frac{1+\sinh(R_0/a_0)}{\cosh(r/a_0)+\cosh(R_0/a_0)} \quad (6)$$

$V_{so}(r)$ is the spin orbit potential [20]:

$$V_{so}(r)=V_{so}\frac{1}{r}\left[\frac{d}{dr}\frac{1}{\left(1+e^{\frac{(r-R_{so})}{a_{so}}}\right)}\right] \quad (7)$$

$V_c(r)$ (for protons only) is Coulomb potential :

$$V_c(r)=\begin{cases}\dfrac{Ze^2}{r} & \text{for} \quad r>R_c\\ \dfrac{Ze^2}{R_c}\left[\dfrac{3}{2}-\dfrac{r^2}{2R_c^2}\right] & \text{for} \quad r\le R_c\end{cases} \quad (8)$$

and $V_c(r)=0$ for neutrons.

The Skyrme force are given by [21]:

$$\begin{aligned}V_{Skyrme}&=\sum_{i<j}V_{ij}=t_0(1+x_0P_\sigma)\delta(\vec{r})\\&+\frac{t_1}{2}(1+x_1P_\sigma)\left[\delta(\vec{r})\vec{k}^2+\vec{k}'^2\delta(\vec{r})\right]\\&+t_2(1+x_2P_\sigma)\vec{k'}.\delta(\vec{r})\vec{k}\\&+\frac{1}{6}t_3(1+x_3P_\sigma)\rho^\alpha(\vec{R})\delta(\vec{r})\\&+it_4\vec{k}'.\delta(\vec{r})(\vec{\sigma}_i+\vec{\sigma}_j)\times\vec{k}\end{aligned} \quad (9)$$

where $P_\sigma, \vec{\sigma}, \delta(\vec{r})$ and $\vec{k}$ are the space exchange operator, Pauli spin matrices vector, delta function pairing force and the relative momentum, respectively and t_0, t_1, t_2, $t_3, x_0, x_1, x_2, x_3, W_0$ and γ are the parameters of Skyrme force.

The charge, as well as the densities of protons or neutrons with the range of the Skyrme HF methodology, are obtained by [22]:

$$\rho_g(\vec{r})=\sum_{\beta\in g}w_\beta\psi_\beta^+(\vec{r})\,\psi_\beta(\vec{r}) \qquad g=n,p,ch \quad (10)$$

where ψ_β is the wave function of a single particle for the state β and $w_\beta$denotes the probability of occupation for the state β.

The nucleus charge distributions ($\rho_{ch}(r)$) can be obtained from the following folding relation [23]:

$$\rho_{ch}(r)=\int\rho_p(r)f_p(r'-r)\,dr' \quad (11)$$

where $\rho_p(r)$ and f_p are the proton density and one proton intrinsic charge distribution, respectively.

Where f_p takes the following form of Gaussian [24]:

$$f_p(r)=\frac{1}{\left(\sqrt{\pi}a_p\right)^3}e^{(-r^2/a_p^2)} \quad (12)$$

The core (R_c), matter (R_m), proton $\left(R_p\right)$ and neutron (R_n) rms radii are obtained by [25]:

$$R_g=\langle r_g^2\rangle^{1/2}=\left[\frac{\int r^2\rho_g(r)dr}{\int\rho_g(r)dr}\right]^{1/2}=c,m,n,p,ch \quad (13)$$

The proton and neutron skin thicknesses are, respectively [26]:

$$\Delta R_p=R_p(Z,N)-R_n(Z,N) \quad (14)$$

$$\Delta R_n=R_n(Z,N)-R_p(Z,N) \quad (15)$$

We have in mirror nuclei with assumed that perfect charge symmetry :

$$R_n(Z,N)=R_p(Z,N) \quad (16)$$

Then, the difference of the proton radii of mirror pair is:

$$\Delta R_{mirror}=R_p(N,Z)-R_p(Z,N) \quad (17)$$

We study the elastic form factors for considered nuclei using the plane wave Born approximation (PWBA) within the proton density distribution $\rho(r)$. In plane wave Born approximation (PWBA), the elastic charge form factor ($F_{ch}(q)$) is given by [27]:

$$F_{ch}(q)=\frac{4\pi}{Z}\int_0^\infty\rho_{ch}(r)j_0(qr)r^2dr \quad (18)$$

where $j_0(qr)$ and q are the Bessel function and the momentum transfer, respectively.

The μ in terms of the M1 operator is defined as :

$$\mu=\sqrt{\frac{4\pi}{3}}\begin{pmatrix}J & 1 & J\\ -J & 0 & J\end{pmatrix}\sum_{t_z}\left|\langle J||\hat{O}(M1)_{t_z}||J\rangle\right|^2\mu_N \quad (19)$$

where μ_N is the nuclear magneton.

In mirror nuclei, the Coulomb energy difference is given by [28]:

$$\Delta E_c = B(N+1,Z) - B(N,Z+1) \quad (20)$$

where $B(N,Z)$ is the binding energy of a nucleus with Z protons and N neutrons.

3. Results and Discussion

In this study, we have been calculated the nuclear proton, neutron and matter densities, the corresponding rms radii, elastic form factors along with the magnetic dipole moments for exotic mirror nuclei ^{17}Ne (S2p=0.933 MeV, τ1/2=109.2 ms) and ^{17}N (S2n=8.374 MeV, τ1/2=4.173 s) [29],[30] using the SHF and SWS calculations. To further support the reliability of the Skyrme Hartree-Fock (SHF) model in our calculations, we employed the LNS5 Skyrme force parametrization. This set of parameters is designed to reproduce key properties of nuclear matter, such as saturation density and symmetry energy. The values of the LNS5 parameters used in our study are listed in Table 1. Each parameter contributes to specific aspects of the nuclear interaction: the central and density-dependent terms control the binding energy and saturation, while the gradient and spin-orbit terms influence the shell structure and density distribution. The accurate reproduction of rms radii, density tails, and magnetic dipole moments in both ^{17}Ne and ^{17}N indicates that the chosen LNS5 parameters provide a suitable description of weakly bound systems. In particular, the role of the spin-orbit interaction is significant in determining the occupation of valence orbits, which directly affects formation of the halo structure. These findings confirm that use of the LNS5 parametrization within the SHF model is effective for investigating the structure of exotic mirror nuclei.

Table 1. The values of the LNS5 parameterization used in SHF Calculations [30].

Parameter	Symbol	Value
Central term coefficient	t_0	-2194.776 MeV·fm³
Gradient term	t_1	482.518 MeV·fm⁵
Gradient term	t_2	138.137 MeV·fm⁵
Density-dependent term	t_3	10784.169 MeV·fm³
Exchange term coefficient	x_0	0.134
Exchange term coefficient	x_1	-0.097
Exchange term coefficient	x_2	-1.399
Exchange term coefficient	x_3	0.171
Spin-orbit strength	W_0	105.674 MeV·fm⁵
Density dependence exponent	γ\gammaγ	0.16667

A core ^{15}O (J^{π},T=1/2$^-$,1/2) plus two-proton valence (J^{π},T=0$^+$,1) is assumed for ^{17}Ne (J^{π},T=1/2$^-$3/2) and a core ^{15}N (J^{π},T=1/2$^-$,1/2) plus two-neutron valence (J^{π},T=0$^+$,1) is assumed for ^{17}N (J^{π},T=1/2$^-$,3/2)).

We assumed that both core nuclei ^{15}O and ^{15}N have the configuration $\{(1s_{1/2})^4, (1p_{3/2})^8, (1p_{1/2})^3\}$. The two-proton valence in ^{17}Ne and two- neutron valence in ^{17}N are assumed to be a pure $2s_{1/2}$ orbit. The results obtained using the Skyrme Hartree Fock (LNS5) and Symmetrized Woods Saxon models show good agreement with experimental data for rms radii, binding energies, and magnetic dipole moments, while also revealing extended density tails characteristic of halo nuclei in ^{17}Ne (proton halo) and ^{17}N (neutron halo). The elastic form factors exhibit distinctive shifts related to the contribution of valence nucleons, and the magnetic dipole moment of ^{17}Ne is excellently reproduced with the REWIL interaction. Overall, these findings confirm the validity of the adopted theoretical models and strengthen the structural interpretation of exotic mirror nuclei.

The results indicate that the mirror nuclei ^{17}Ne and ^{17}N exhibit clear signatures of halo structures through both quantitative and qualitative indicators.

The calculations reveal an enhancement in the rms matter radii compared with their core nuclei, along with deviations in the matter-to-charge radius ratio, extended low-density tails in the density distributions, and distinct shifts in the minima of the elastic form factors.

These observations, further supported by the magnetic dipole moment analysis, confirm the existence of a proton halo in ^{17}Ne and a neutron halo in ^{17}N, consistent with the established systematics of halo nuclei.

Table 2. The SWS parameters.

Nuclei	V_0 (MeV)		Vso (MeV)	a_0= aso (fm)	r_0= rso (fm)	r_c (fm)
	Core	Valence				
^{17}Ne	66.785	50.850	6.0	0.646	1.288	1.464
^{17}N	64.785	46.33	6.0	0.546	1.288	1.464
^{21}Ne	60.834		6.0	0.638	1.282	1.381
^{15}N	50.871		6.0	0.577	1.292	1.422

Table 2. displays the values of the SWS parameters utilized in the present calculations for selected nuclei. The depth of SWS potential (V_0) of core nuclei provides the single particle energies of Ref. [31] whereas the V_0 for valence proton (valence neutron) in ^{17}Ne (in ^{17}N) and other parameters provide the matter rms radii of exotic nuclei and experimental (theoretical of Ref. [32] $\varepsilon_{n\ell j}$ of last proton (neutron). The calculated $\varepsilon_{n\ell j}$ for proton and neutron is listed in Table 3.

The calculated rms radii of core (R_c), matter (R_m), proton (R_p) and neutron (R_n) densities obtained by SHF and SWS calculations are compared in Table 4. with the experimental results [33]-[37] .A remarkable agreement has been shown between the calculated and experimental results with both calculations in Tables 4 and 5.

Table 6. shows the calculated proton skin of halo nucleus ^{17}Ne and the neutron-skin of its mirror nucleus ^{17}N as well as the difference of proton radii for these mirror pair obtained by SHF and SWS calculations. It can be seen from Table 5 and 6 that the proton skin of the proton-rich nucleus ^{17}Ne is larger than the neutron skin of its mirror neutron-rich nucleus ^{17}N. This is attributed to the Coulomb repulsion of protons. The theoretical B.E and ΔE_c of ^{17}Ne and ^{17}N in Table 7. together with experimental data . It is found that the calculated results agree reasonably with the experimental ones. The Coulomb Displacement Energy (CDE) values were calculated from the differences in the binding energies of the mirror nuclei ^{17}Ne and ^{17}N, following the standard definition. We clarify that the use of the Plane-Wave Born Approximation (PWBA) for the elastic form factor calculations is justified by the fact that the studied nuclei ^{17}Ne and ^{17}N are relatively light systems, where distortion effects and relativistic corrections are expected to be small compared to heavier or deformed nuclei. The observed differences in skin thickness and form factor minima between ^{17}Ne and ^{17}N are not purely numerical. The pronounced proton skin in ^{17}Ne arises due to Coulomb repulsion, which drives the valence protons to spatially extend further from the nuclear core, enhancing the halo feature. Conversely, the absence of such repulsion in ^{17}N allows the two weakly bound neutrons to form an extended low-density neutron tail, supported by occupation of the $2s_{1/2}$ orbital. These physical phenomena underscore the quantum mechanical origins of the halo effect, reinforced by the calculated root-mean-square radii and form factors.

Table 3. The calculated .

Nuclei	$n\ell_j$	Proton			Neutron	
		ε_{cal}(MeV)	ε(MeV)	$\varepsilon_{exp.}$(MeV)	ε_{cal}(MeV)	ε(MeV)
^{17}Ne	1s1/2	-40.359	-40.359		-45.042	-45.042
	1p3/2	-25.459	-25.459		-29.846	-29.846
	1p1/2	-22.228	-22.228		-26.624	-26.624
	2s1/2	-0.466		-0.466		
^{17}N	1s1/2	-41.688	-41.688		-47.440	-47.440
	1p3/2	-26.824	-26.824		-34.535	-34.535
	1p1/2	-23.567	-23.567		-32.199	-32.199
	2s1/2				-1.963	-1.963

The calculated μ moment for ^{21,17}Ne and ^{15,17}N isotopes are presented in Table 8 together with the experimental data [38]. These calculations are performed using ZBM-model space with different interactions labeled as ZBMI, ZBMII [39], REWIL and ZWM [40], which are carried out via the NuShellX@MSU code.

The free-nucleon g factors have been used to evaluate μ moment. It is obvious from Table 8. the measured value of the ^{17}Ne (0.787±0.014) is excellent reproduced with REWIL interaction in sign and magnitude (0.789). All calculated values of ^{21}Ne are underestimated experimental value (-0.661±0.005). Calculations predict a negative sign as the experimental result. All calculated

values of ^{17}N agree well with the measured value (0.355±0.004) but with an opposite sign. The calculated value of ^{15}N obtained by ZWM interaction (-0.339) is closer to the experimental value (-0.283±0.005) with correct sign.

In Figs. 1(a)-(d) we present the calculated matter densities (dashed red curves) calculated with both SHF (upper part) and SWS (lower part) calculations for exotic mirror ^{17}Ne [Figs. 1(a) and 1(c)] and ^{17}N [Figs. 1(b) and 1(d)]. The calculated densities of ^{17}Ne are compared with experimental data (grey area) taken from Ref. [40].

Table 4. The calculated $R_c$and R_m rms radii and experimental ones.

Nuclei	R_c			R_m		
	SHF	**SWS**	**Exp.** [37]	**SHF**	**SWS**	**Exp.** [38],[39]
^{17}Ne	2.48	2.44	2.44±0.04	2.85	2.84	2.84±0.23
^{17}N	2.46	2.42	2.42±0.1	2.82	2.79	2.79±0.04

Table 5. The calculated R_p and R_n rms radii and experimental ones.

Nuclei	R_p			R_n		
	SHF	**SWS**	**Exp.** [40]	**SHF**	**SWS**	**Exp.**
^{17}Ne	3.05	3.10	------	2.54	2.42	-----
^{17}N	2.54	2.42	2.43±0.05	3.00	3.02	2.92±0.04

Table 6. Calculated ΔR_p, ΔR_n and $\Delta R_{mirror}$of ^{17}Ne and ^{17}N.

Nucleus	ΔR_p		Mirror	ΔR_n		ΔR_{mirror}	
	SHF	**SWS**		**SHF**	**SWS**	**SHF**	**SWS**
^{17}Ne	0.51	0.68	^{17}N	0.46	0.60	-0.51	-0.68

Table 7. The B.E and ΔE_c of ^{17}Ne and ^{17}N.

Nucleus	$B.E_{the.}$	$B.E_{exp.}$ [33]	Mirror	$B.E_{the.}$	$B.E_{exp.}$ [33]	ΔE_c	$\Delta E_c(exp)$
^{17}Ne	103.06	112.9	^{17}N	113.22	123.87	10.13	10.97

Table 8. Calculated and experimental results of μ moment.

Nuclei	ZBMI	ZBMII	REWIL	ZWM	Exp.
^{17}Ne	0.813	0.754	0.789	0.728	0.787±0.014
^{21}Ne	-0.324	-0.211	-0.194	-0.266	-0.661±0.005
^{17}N	-0.430	-0.374	-0.403	-0.350	0.355±0.004
^{15}N	-0.526	-0.430	-0.368	-0.339	-0.283±0.005

Due to the absence of the available experimental data of ^{17}N nucleus, the calculated results of this nucleus are compared with theoretical results of Ref. [36] given by dotted symbols. In Fig. 1 the black and blue curves represent the calculated results of the core and valence densities, respectively. From Figs. 1 it is obvious that the calculated density distribution of ^{17}Ne has a long density tail which consistent with the experimental one. From Figs. 1 we note that the calculated results are agree well with the dotted symbols. In Figs. 2(a)-(d) the neutron (black curve) and proton (blue curve) densities of the ^{17}Ne and ^{17}N are compared with each other. From Figs. 2(a) and 2(c) we note that, the proton densities of ^{17}Ne have a long tail with respect to the neutron densities. On the contrary, from Figs. 2 we note that the neutron densities of ^{17}N have a long tail with respect to the proton densities. From the above results, it can be seen that the two protons halo appears in ^{17}Ne when the outer two proton occupy the 2s1/2 orbit. Meanwhile, the two neutrons halo appears in ^{17}N when the outer two neutron occupy the 2s1/2 orbit. Figs. 3(a)-(d) compare the calculated results of matter densities for unstable ^{17}Ne and ^{17}N (dashed-red distributions) and stable ^{21}Ne and ^{15}N (black distributions) isotopes. From these figures, we can observe that, there is a difference in the behavior of the black and dashed-red distributions. This demonstrates a long tail in dashed red distributions and supports the halo structure of ^{17}Ne and ^{17}N nuclei.

.

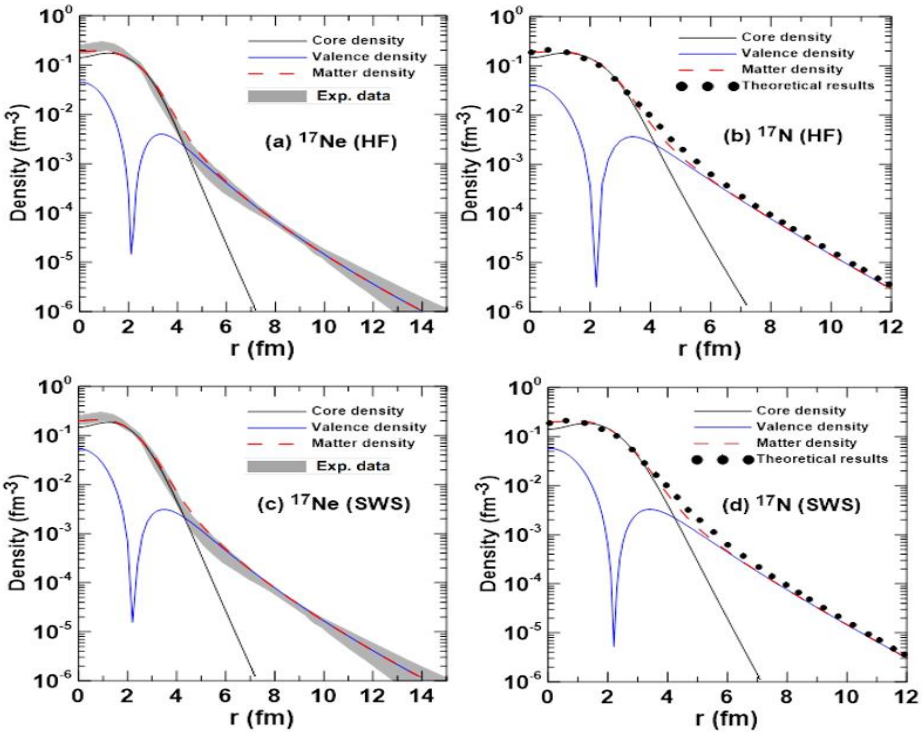

Figure 1. The core density $\rho_c(r)$, halo density $\rho_h(r)$, and matter density $\rho_m(r)$ of the mirror nuclei ^{17}Ne and ^{17}N.

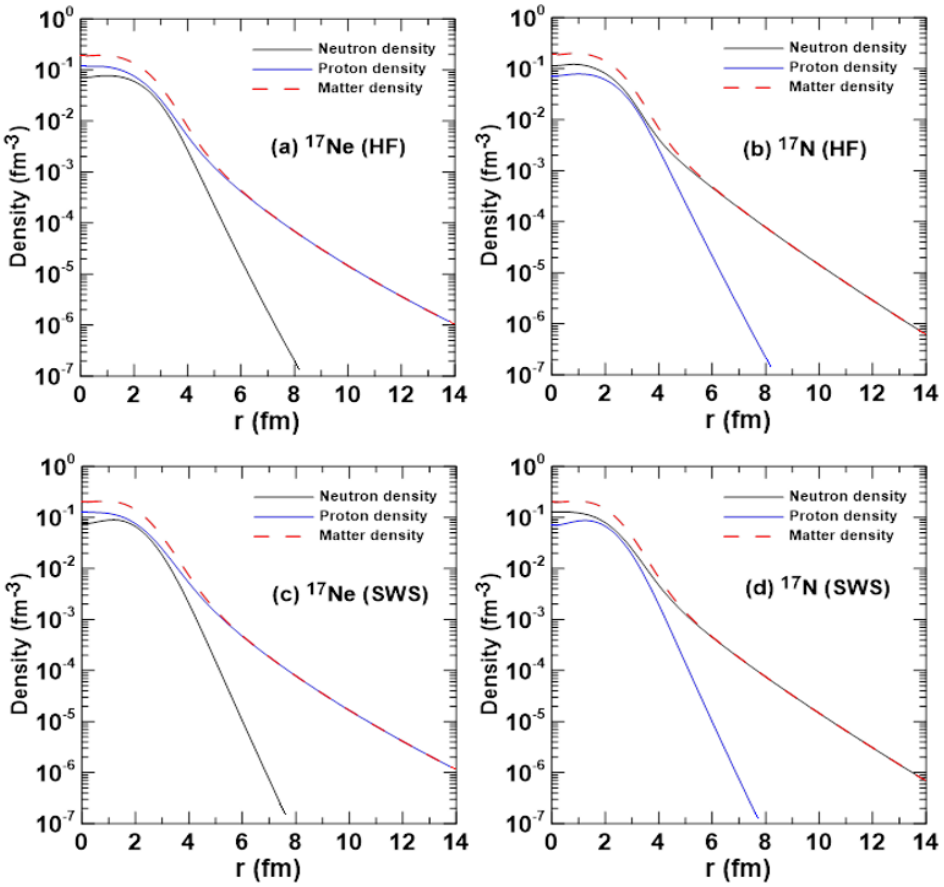

Figure 2. The neutron density $\rho_n(r)$, proton density $\rho_p(r)$, and matter density $\rho_m(r)$ of the mirror nuclei ^{17}Ne and ^{17}N.

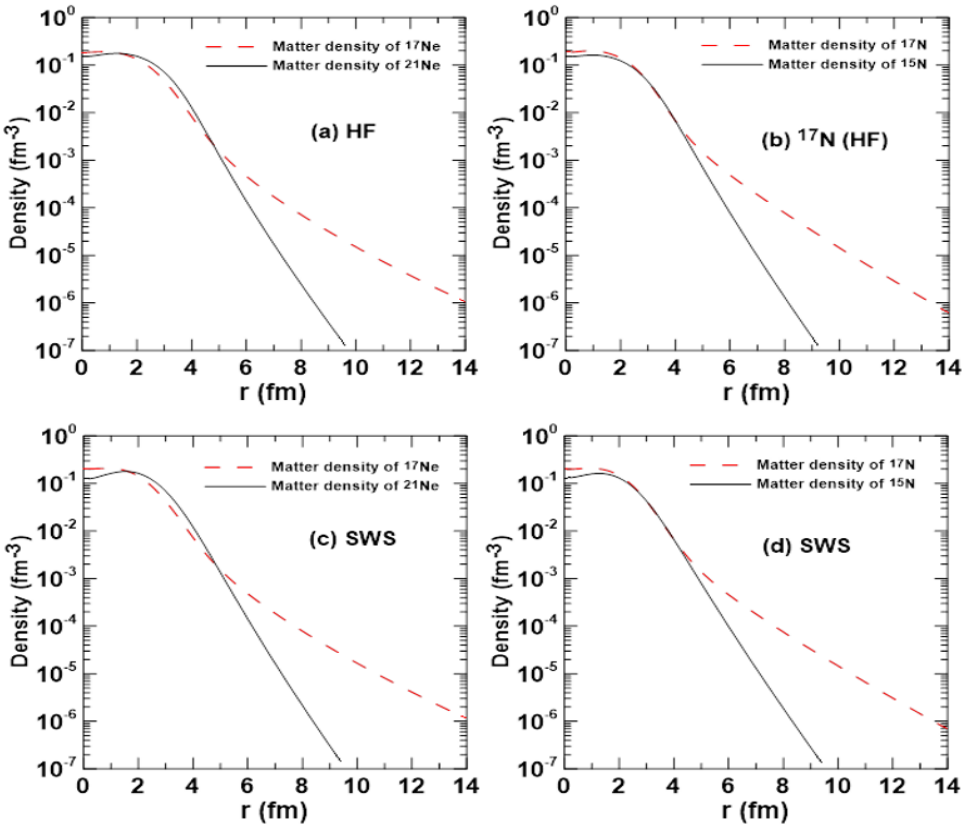

Figure 3. The matter density ρ_m (r) of the isotopes ^{21,17}Ne and ^{15,17}N.

Figs. 4(a)-(d) depicted the calculated results of the C_0 charge form factors for ^{21,17}Ne (left panel) and ^{15,17}N (right panel) isotopes calculated by SHF and SWS calculations using the PWBA.

The blue and red curves refer to C_0 of unstable and stable isotopes, respectively.

For comparison the experimental $F_{ch}(q)$ for stable isotopes ^{21}Ne and ^{15}N are given by dotted symbols. The agreement is shown to be very well between the theoretical and experimental results of ^{21}Ne and ^{15}N. It is obvious that there is one minimum in both blue and red curves. One can see from Figs. 4(a) and 4(c), the shift of the minima to larger values of q is a common property of the blue curves. This is attributed to the influence of the charge density distributions of the last two-proton in ^{17}Ne.

On the contrary, the shift of the minima to smaller values of q is a common property of the blue curves as shown in Figs. 4(b) and 4(d). This change is attributed to the coupling of the two extra neutrons to the core ^{15}N which lead to pull the charge density out.

The comparison between halo nuclei and their stable isotopes (^{21}Ne and ^{15}N), as illustrated in Figs. 3 and 4, is essential to highlight the impact of valence nucleon configurations on the spatial extension of nuclear matter distributions.

This contrast not only underscores the presence of extended density tails in halo systems but also serves to validate the applied theoretical models by demonstrating their sensitivity to structural differences. The selection of ^{21}Ne and ^{15}N as reference nuclei is deliberate, given their well-established stability and availability of experimental data, which provide a solid baseline for interpreting the deviations observed in the exotic nuclei ^{17}Ne and ^{17}N. Hence, the comparative analysis is a critical component of the structural interpretation, not merely illustrative.

4. Conclusions

The ground state properties like the nuclear densities and the rms radii of exotic mirror nuclei ^{17}Ne and ^{17}N have been investigated in the framework of the SHF and SWS calculations.

The evaluated results are compared with available experimental data. It found that a common feature of the matter densities for above selected exotic nuclei is the long tail behavior. The elastic form factors for ^{21,17}Ne and ^{17,15}N isotopes have been also studied using the PWBA. It is found that, the shift of the minima to larger values of q is a common property of the form factors for ^{17}Ne.

This is attributed to the influence of the charge density distributions of the last two-proton in ^{17}Ne. On the contrary, the shift of the minima to smaller values of q is a common property of the form factors for ^{17}N. This change is attributed to the coupling of the two extra neutrons to the core ^{15}N which lead to pull the charge density out.

The μ moments for above selected nuclei have been also calculated. It is found that the theoretical and experimental results of μ moments agree reasonably for all selected nuclei.

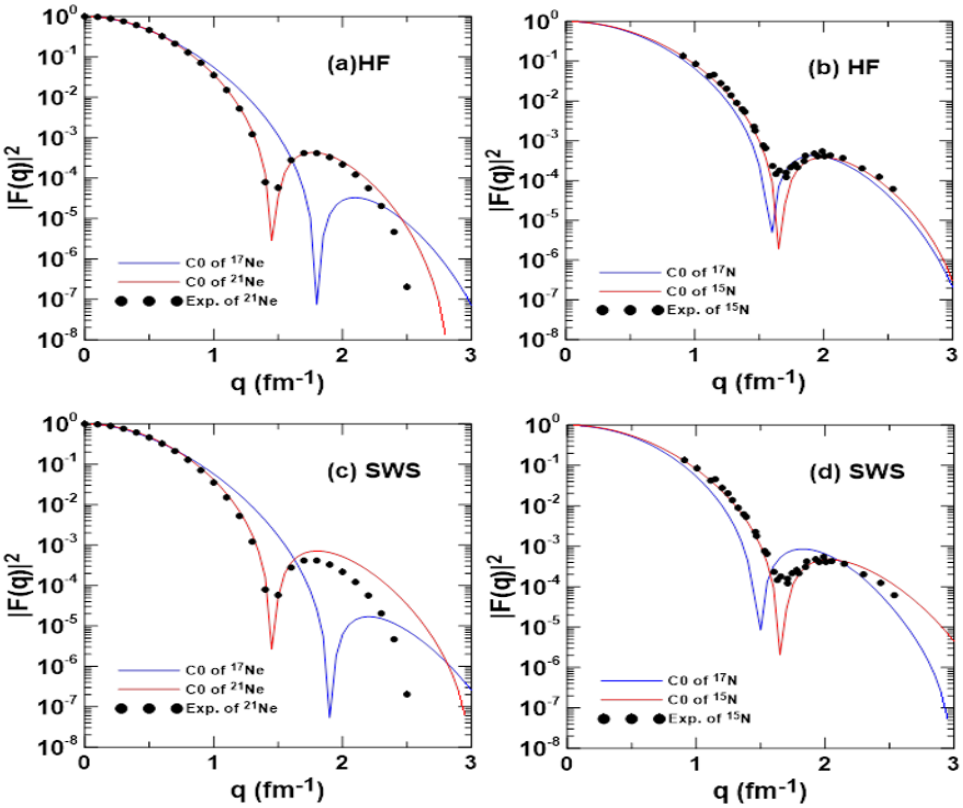

Figure 4. The C_0 charge form factors of the isotopes ^{21,17}Ne and ^{15,17}N.

These findings contribute to the broader understanding of nuclear structure in weakly bound systems and validate the predictive capability of SHF and SWS models for exotic mirror nuclei. The results hold promise for application in the design of future electron–radioactive ion beam scattering experiments and could guide experimentalists in choosing appropriate observables to probe halo signatures. Additionally, the detailed analysis of magnetic dipole moments and form factor shifts may serve as a foundation for refining nuclear interaction models in regions near the drip lines.

Authors Contribution

All the authors have participated sufficiently in the intellectual content, conception and design of this work or the analysis and interpretation of the data (when applicable), as well as the writing of the manuscript.

Availability of data and materials

The data that support the findings of this study are available from the corresponding author, upon reasonable request.

Conflict of interests

The author states that there is no conflict of interest.

References

[1] A. N. Abdullah, "The ground state properties of some exotic nuclei studied by the two-body model," *International Journal of Modern Physics E*, vol. 31, no. 08, p. 2250076, 2022, doi.org/10.1142/S0218301322500768

[2] H. K. Mahdi and A. N. Abdullah, "Retraction: Matter density distributions of halo 9C and 12N nuclei," in *AIP Conference Proceedings*, 2023, vol. 2977, no. 1, p. 040118, doi.org/10.1063/5.0182532

[3] S. Q. Abdullah and A. N. Abdullah, "Matter density distributions and reaction cross sections for ^{8}Li and ^{22}N exotic nuclei," *Iraqi Journal of Science, vol, 63, no, 3,* pp. 1030–1038, 2022, doi.org/10.1007/s40995-019-00799-x

[4] A. N. Abdullah, "Systematic Study of the Nuclear Structure for Some Exotic Nuclei Using Skyrme–Hartree–Fock Method," *Iranian Journal of Science and Technology, Transactions A: Science*, vol. 44, no. 1, pp. 283–288, 2020, doi.org/10.24996/ijs.2022.63.3.12

[5] M. Aygun, "Double-folding analysis of the ^{6}Li^{+} ^{58}Ni reaction using the ab initio density distribution," *The European Physical Journal A*, vol. 48, no. 10, p. 145, 2012, doi.org/10.1140/epja/i2012-12145-y

[6] B. Blank *et al.*, "Total interaction and proton-removal cross-section measurements for the proton-rich isotopes ^{7}Be, ^{8}B, and ^{9}C," *Nuclear Physics A*, vol. 624, no. 2, pp. 242–256, 1997, doi.org/10.1016/S0375-9474(97)81837-4

[7] S. Ilieva *et al.*, "Nuclear-matter density distribution in the neutron-rich nuclei $^{12, 14}$Be from proton elastic scattering in inverse kinematics," *Nuclear Physics A*, vol. 875, pp. 8–28, 2012 , doi.org/10.1016/j.nuclphysa.2011.11.010

[8] R. Hofstadter, "Electron scattering and nuclear structure," *Reviews of Modern Physics*, vol. 28, no. 3, p. 214, 1956,

doi.org/10.1103/RevModPhys.28.214

[9] C. Batty, E. Friedman, H. Gils, and H. Rebel, "Experimental methods for studying nuclear density distributions," in *Advances in Nuclear Physics*: Springer, pp. 1–188, 1989, doi.org/10.1007/978-1-4613-9907-0_1

[10] B. Brown, W. Richter, and R. Lindsay, "Displacement energies with the Skyrme Hartree–Fock method," *Physics Letters B*, vol. 483, no. 1-3, pp. 49–54, 2000, doi.org/10.1016/S0370-2693(00)00589-X

[11] S. Lenzi *et al.*, "Isospin symmetry breaking in mirror nuclei ^{23}Mg-^{23}Na," 2017, doi:10.24996/ijs.2018.59.2B.5

[12] R. A. Mohammed and W. Z. Majeed, "Exotic structure of ^{17}Ne-^{17}N and ^{23}Al-^{23}Ne mirror nuclei," *East European Journal of Physics*, no. 4, pp. 72–79, 2022, doi.org/10.26565/2312-4334-2022-4-05

[13] K. Heyde, P. von Neumann-Cosel, and A. Richter, "Magnetic dipole excitations in nuclei: Elementary modes of nucleonic motion," *Reviews of Modern Physics*, vol. 82, no. 3, pp. 2365–2419, 2010, doi.org/10.1103/RevModPhys.82.2365

[14] M.-Q. Ding, D.-Q. Fang, and Y.-G. Ma, "Neutron skin and its effects in heavy-ion collisions," *Nuclear Science and Techniques*, vol. 35, no. 12, p. 211, 2024, doi.org/10.1007/s41365-024-01584-1

[15] H. K. Mahdi and A. N. Abdullah, "Elastic Form Factors and Matter Density Distributions of Some Neutron-Rich Nuclei," *Iraqi Journal of Physics*, vol. 20, no. 4, pp. 18–27, 2022, doi.org/10.30723/ijp.v20i4.1013

[16] S. F. Hadi and A. K. Hasan, "Calculate the nuclear structure for the $^{72, 74, 76}$Kr isotopes by using NuShellX@ MSU code," *Journal of Theoretical and Applied Physics*, vol. 19, no. 3, 2025, doi: 10.57647/j.jtap.2025.1903.28

[17] C. Forssén, G. Hagen, M. Hjorth-Jensen, W. Nazarewicz, and J. Rotureau, "Living on the edge of stability, the limits of the nuclear landscape," *Physica Scripta*, vol. 2013, no. T152, p. 014022, 2013, doi: 10.1088/0031-8949/2013/T152/014022

[18] Wang Meng *et al.*, "Configuration of the valence neutrons of ^{17}B", vol, 32, no, 7, 548, 2008, doi: 10.1088/1674-1137/32/7/007

[19] M. Grypeos, G. Lalazissis, S. Massen, and C. Panos, "The'cosh'or symmetrized Woods-Saxon nuclear potential," *Journal of Physics G: Nuclear and Particle Physics*, vol. 17, no. 7, p. 1093, 1991, doi: 10.1088/0954-3899/17/7/008

[20] Y. Chu, Z. Ren, and C. Xu, "Properties of proton-rich nuclei in a three-body model," *The European Physical Journal A*, vol. 37, no. 3, pp. 361–366, 2008, doi.org/10.1140/epja/i2008-10626-2

[21] G. Lingxiao, Z. Yizhong, and W. Nörenberg, "Temperature-dependent optical potential and mean free path based on skyrme interactions," *Nuclear Physics A*, vol. 459, no. 1, pp. 77–92, 1986 doi.org/10.1016/0375-9474(86)90057-6

[22] S. Goriely, M. Samyn, J. Pearson, and M. Onsi, "Further explorations of Skyrme–Hartree–Fock–Bogoliubov mass formulas. IV: Neutron-matter constraint," *Nuclear Physics A*, vol. 750, no. 2-4, pp. 425–443, 2005, doi.org/10.1016/j.nuclphysa.2005.01.009

[23] L. Guo-Qiang, "A systematic study of nuclear properties with Skyrme forces," *Journal of Physics G: Nuclear and Particle Physics*, vol. 17, no. 1, p. 1, 1991, doi: 10.1088/0954-3899/17/1/002

[24] A. N. Abdullah, "Investigation of halo structure of neutron rich ^{14}B, ^{15}C, ^{19}C and ^{22}N nuclei in the two body model," *International Journal of Modern Physics E*, vol. 29, no. 03, p. 2050015, 2020, doi.org/10.1142/S0218301320500159

[25] R. Baldik, H. Aytekin, and E. Tel, "Investigation of neutron and proton distributions of He, Li, and Be isotopes using the new Skyrme-force parameters," *Physics of Atomic Nuclei*, vol. 73, no. 1, pp. 74–81, 2010, doi: 10.1134/S1063778810010096

[26] M. Gaidarov, I. Moumene, A. Antonov, D. Kadrev, P. Sarriguren, and E. M. De Guerra, "Proton and neutron skins and symmetry energy of mirror nuclei," *Nuclear Physics A*, vol. 1004, p. 122061, 2020, doi.org/10.1016/j.nuclphysa.2020.122061

[27] A. Antonov, M. Gaidarov, D. Kadrev, P. Hodgson, and E. M. De Guerra, "Charge density distributions and related form factors in neutron-rich light exotic nuclei," *International Journal of Modern Physics E*, vol. 13, no. 04, pp. 759–772, 2004 , doi.org/10.1142/S0218301304002430

[28] B. Agrawal, T. Sil, S. Samaddar, J. De, and S. Shlomo, "Coulomb energy differences in mirror nuclei revisited," *Physical Review C*, vol. 64, no. 2, p. 024305, 2001, doi.org/10.1103/PhysRevC.64.024305

[29] Audi G. et al., "The NUBASE2016 evaluation of nuclear properties," *Chinese physics C*, vol. 41, no. 3, p. 030001, 2017, doi: 10.1088/1674-1137/41/3/030001

[30] M. Wang, W. J. Huang, F. G. Kondev, G. Audi, and S. Naimi, "The AME 2020 atomic mass evaluation (II). Tables, graphs and references," *Chinese Physics C*, vol. 45, no. 3, p. 030003, 2021, doi: 10.1088/1674-1137/abddaf

[31] B. Brown and W. Rae, "The shell-model code NuShellX@ MSU," *Nuclear Data Sheets*, vol. 120, pp. 115–118, 2014, doi.org/10.1016/j.nds.2014.07.022

[32] Z. Hu-Yong *et al.*, "Structures of ^{17}F and ^{17}O, ^{17}Ne and ^{17}N inthe Ground State and the First Excited State," *Chinese physics letters*, vol. 20, no. 9, p. 1462, 2003, doi: 10.1088/0256-307X/20/9/315

[33] A. Ozawa, T. Suzuki, and I. Tanihata, "Nuclear size and related topics," *Nuclear Physics A*, vol. 693, no. 1-2, pp. 32–62, 2001,

doi.org/10.1016/S0375-9474(01)01152-6

[34] R. Warner *et al.*, "Reaction and proton-removal cross sections of ^{6}Li, ^{7}Be, ^{10}B, ^{11,10,9}C, ^{12}N, ^{15,13}O, and ^{17}Ne on Si at 15 to 53 MeV/nucleon," *Physical Review C—Nuclear Physics*, vol. 74, no. 1, p. 014605, 2006, doi.org/10.1103/PhysRevC.74.01460

[35] S. Ahmad, A. Usmani, and Z. Khan, "Matter radii of light proton-rich and neutron-rich nuclear isotopes," *Physical Review C*, vol. 96, no. 6, p. 064602, 2017, doi.org/10.1103/PhysRevC.96.064602

[36] A. Ozawa *et al.*, "Interaction cross sections and radii of the mass number A= 17 isobar (^{17}N, ^{17}F, and ^{17}Ne)," *Physics Letters B*, vol. 334, no. 1-2, pp. 18–22, 1994, doi.org/10.1016/0370-2693(94)90585-1

[37] E. Liatard *et al.*, "Matter distribution in neutron-rich light nuclei and total reaction cross-section," *Europhysics Letters*, vol. 13, no. 5, p. 401, 1990, doi: 10.1209/0295-5075/13/5/004

[38] N. Stone, A. Stuchbery, and P. Dimitriou, "Evaluation of Nuclear Moments," International Atomic Energy Agency, International Nuclear Data Committee …, 2017, doi.org/10.1006/adnd.1995.1007

[39] A. Zuker, B. Buck, and J. McGrory, "Structure of O 16," *Physical Review Letters*, vol. 21, no. 1, p. 39, 1968, doi.org/10.1103/PhysRevLett.21.39

[40] J. McGrory and B. Wildenthal, "Shell-model calculations for A= 18, 19, and 20 nuclei with core excitation included explicity," *Physical Review C*, vol. 7, no. 3, p. 974, 1973 , doi.org/10.1103/PhysRevC.7.974